LOW ENERGY EARTH-MOON TRANSFER THROUGH THE LAGRANGIAN EQUILIBRIUM POINTS

Cristiano Fiorilo de Melo
Instituto Nacional de Pesquisas Espaciais - INPE, CP 515, São José dos Campos, SP, Brazil
e-mail cristianofiorilo@terra.com.br

Elbert Einstein Nherer Macau
Instituto Nacional de Pesquisas Espaciais - INPE, CP 515, São José dos Campos, SP, Brazil
Email elbert@lac.inpe.br

Othon Cabo Winter
Grupo de Dinâmica Orbital e Planetologia - UNESP, CP 205, Guaratinguetá, SP, 12500-000, Brazil
e-mail ocwinter@feg.unesp.br

Ernesto Vieira Neto
Grupo de Dinâmica Orbital e Planetologia - UNESP, CP 205, Guaratinguetá, SP, 12500-000, Brazil
e-mail ernesto@feg.unesp.br

Abstract. *The lunar sphere of influence, whose radius is some 66300km, has regions of stable orbits around the Moon and also regions that contain trajectories which, after spending some time around the Moon, escape and are later recaptured by lunar gravity. Both the escape and the capture occur along the Lagrangian equilibrium points L1 and L2. In this study, we mapped out the region of lunar influence considering the restricted three-body Earth-Moon-particle problem and the four-body Sun-Earth-Moon-particle (probe) problem. We identified the stable trajectories, and the escape and capture trajectories through the L1 and L2 in plots of the eccentricity versus the semi-major axis as a function of the time that the energy of the osculating lunar trajectory in the two-body Moon-particle problem remains negative. We also investigated the properties of these routes, giving special attention to the fact that they supply a natural mechanism for performing low-energy transfers between the Earth and the Moon, and can thus be useful on a great number of future missions.*

Keywords*: Astrodynamics; Earth-Moon Transfer, Mission Design, Orbital Maneuvers.*

1. INTRODUCTION

Generally, a lunar trajectory is initially planned based on the Hohmann or Patched-conic approximations (Bate *et al.*, 1971). Both are completely described by the dynamics of the two-body, Earth-vehicle on takeoff, and Moon-vehicle on arrival and capture by the Moon. Keeping in mind the differences between these two transfers, we can say from an analytical standpoint that they require two impulses. The first impulse transfers the ship from a terrestrial parking orbit to a geocentric transfer ellipsis of high eccentricity towards the Moon The second impulse is applied to stabilize the vehicle in a circular orbit around the Moon exactly when it reaches the altitude planned for this orbit. From the practical standpoint, there is always a need to apply a midway impulse to correct deviations caused to the transfer trajectory by the effect of the Sun's and Moon's gravitational fields. The sum of the magnitudes of these three $\Delta\mathbf{V}$ exceeds 4.000km/s, and typical flight time (TOF) of these transfers is approximately 5 days. The dynamics of the two-body problem do not allow gains in inclination without the application of extra impulses for this purpose. But, in spite of some limitations, the two methods provide the first analytic approximation for an Earth-Moon transfer.

The transfers between the Earth and the Moon can also be considered in the context of the restricted three-body problem (R3BP). By doing so, because of the richness of the dynamics of this system, several different approaches have been proposed over the years. As example, we can mention the analytical and numerical works of Arenstorf (1963a, 1963b), Arenstorf and Davidson (1963) and Davidson (1964), that exploit special trajectories of the R3BP with small mass ratio that pass near the primary bodies and whose periods are commensurable with the primary with small mass (the Moon, for instance). Belbruno (1987) and Belbruno and Miller (1990, 1993) introduced the bases for low-energy lunar transfers through the mechanism of ballistic capture through the Hill regions based on the dynamics of the restricted three-body Sun-Earth-particle problem and the Earth-Moon-particle problem. In 1991, the mission by Japanese lunar probe Muses-A, renamed Hiten, was saved with the application of these new techniques (Belbruno and Miller, 1990). Since then, this approach has been much explored in the literature; see for example, Koon *et al.* (2000, 2001), Villac and Scheeres (2003), Dahlke (2003) and Macau and Grebogi (2006). Transfers involving ballistic capture offer significant reduction in ΔV_{Total} of the maneuver, but they require longer times.

In this work, we consider another approach to get low-energy transfer from Earth to the Moon: we explored the Moon's sphere of influence, whose radius is approximately 66300km, considering the restricted three-body Earth-Moon-particle problem, R3BP, and investigated the evolutions of the trajectories whose periseleniums, in $t = 0$, are

located between the Moon and L1, and between the Moon and L2 (Fig. 1). In this way, it is possible to identify, within the lunar sphere of influence, regions of direct stable orbits around the Moon that are derived from the periodic orbits of the Family H2 (Broucke, 1968) and of the quasi-periodic orbits that oscillate around them, which have already been described by Winter and Vieira Neto (2002). We also identified regions containing trajectories which, after remaining around the Moon for some time, escape through L1 or L2, and later are recaptured by the lunar gravitational field (ballistic capture). These last two types of trajectories define at least four natural escape and capture routes by the Moon. Two of these routes are defined by the trajectories that first escape from the Moon through L1 to area around the Earth and later are also recaptured by the Moon's gravitational field through L1. These are the escape and capture internal routes, respectively. Similarly, the other two routes are defined by those trajectories that escape from the Moon through L2 to area beyond the Earth-Moon System and after are recaptured by the Moon also through L2. These are, therefore, the external routes of escape and capture, respectively. All four routes mentioned penetrate each other in the lunar sphere of influence. We classified these routes based on the sets of value of their Jacobi constants, C_J. Thus, with this investigation, we are able to present the region within the sphere of influence of the Moon through maps (Fig. 2 and 4) in plots of the eccentricity versus the semi-major axis, as a function of the time that the energy of the osculating lunar trajectory, in the two-body Moon-particle problem, remains negative, that is, as a function of the capture time. In practical terms, this allows us to choose the best transfer and capture trajectory for a specific mission, thus minimizing costs. This is possible because a probe placed in one convenient capture trajectory can be led naturally to a lunar orbit without the need for the application of insertion impulses and would remain captured for periods that would be sufficient to complete a vast number of missions. Besides, these trajectories can be transferred to stable orbits with the application of a small ΔV, and then remain around the Moon for 1000 days. For this reason, we investigated ways to acquire these trajectories, however, unlike Belbruno and Miller (1993) and Koon *et al.* (2000, 2001), we opted to conduct the probe to the capture routes through intermediate trajectories conceived initially with geocentric ellipses, but which in fact serve as a reference for the construction of intermediary trajectories in the three and four-body problems.

In order to verify the robustness of the routes, we investigated the evolutions of the trajectories, considering a more complex and realistic system, the four-body Sun-Earth-Moon-particle problem, which takes into account, in addition to the mutual attractions among the bodies, the eccentricity of the Earth's orbit, the eccentricity and inclination of the Moon's orbit. Even so, the routes continue to exist, but with evolution in three-dimensional space. In spite of the loss of analytical solutions, which also occurs for the R3BP, the orbital parameters of the trajectories can be defined as a variation of an osculating Keplerian orbit. On the other hand, even being governed by Newton's law of gravitational attraction, the two dynamical systems considered present chaotic behavior, a fact that also can be examined during the acquisition of these trajectories and during the final trip to the Moon, applying targeting techniques and control chaos (Macau and Grebogi, 2006) to reduce the transfer time even more.

2. DYNAMICAL SYSTEMS

2.1. The Restricted Three-body Earth-Moon-Particle Problem R3BP

This problem can be defined by considering the Earth, with mass M_{Earth}, and the Moon, with mass M_{Moon}, called primaries, and a particle of very small mass in relation to the primaries so that it does not influence their motion. Furthermore, the primaries move in circular and coplanar orbits about their common centre of mass. The particle motion occurs in the plane defined by Earth and the Moon orbits and under their gravitational attraction. These hypotheses permit us to introduce a system of coordinates, called synodic system, in which the primaries M_{Earth} and M_{Moon} remain fixed over the *x* axis. This system can be normalized considering its reduced mass μ, as unitary mass, that is, $\mu = \mu_{Earth} + \mu_{Moon} = 1$, with $\mu_{Earth} = M_{Earth}/(M_{Earth}+M_{Moon}) = 0.9878494$ and $\mu_{Moon} = M_{Moon}/(M_{Earth}+M_{Moon}) = 0.0121506$. The constant distance between the Earth and Moon (384400km) is also considered the unit of length, thus their coordinates are $(-\mu_{Moon}, 0)$ and $(\mu_{Earth}, 0)$, respectively. The mean motion *n* of M_{Earth} and M_{Moon} is considered equal to 1, and, therefore, their orbital period around the center of mass is equal to 2π, and the unit of time is 4.348days. In this system, the particle equations of motion can be uncoupled from the primaries, and given in components, in this system by (e. g. Murray and Dermott, 1999)

$$\ddot{x} - 2\dot{y} - x = -\left[\mu_{Earth} \frac{x + \mu_{Moon}}{r_{EP}^3} + \mu_{Moon} \frac{x - \mu_{Earth}}{r_{MP}^3} \right], \qquad (1.a)$$

$$\ddot{y} + 2\dot{x} - y = -\left[\frac{\mu_{Earth}}{r_{EP}^3} + \frac{\mu_{Moon}}{r_{MP}^3} \right] y , \qquad (1.b)$$

where $r_{EP} = [(x + \mu_{Moon})^2 + y^2]^{1/2}$ and $r_{MP} = [(x - \mu_{Earth})^2 + y^2]^{1/2}$ are the distances between the Earth and particle, and Moon and particle, respectively. In this system the energy and the angular momentum are not conserved.

The R3BP has five equilibrium points, known as Lagrangian points. Three of them, L1, L2 and L3 are aligned with the primaries and called collinear or Euclerian points; the other two points, L4 and L5, are at the vertex of two equilateral triangles with the primaries and are called triangular points (Fig. 1).

The R3BP has a first integral of motion called the Jacobi integral, or simply Jacobi constant, C_j, given by

$$C_j = x^2 + y^2 + 2\left(\frac{\mu_{Earth}}{r_{EP}} + \frac{\mu_{Moon}}{r_{MP}}\right) - \dot{x}^2 - \dot{y}^2 .$$ (2)

Putting $\dot{x}^2 + \dot{y}^2 = 0$ for a given value of C_j, Eq. (2) defines the zero velocity curves, and can be interpreted as the borders that limit the regions of this plane that are free or forbidden for the particle to move in.

Figure 1 also shows the zero velocity curves for $C_j = C_j(L1)$, $C_j = C_j(L2)$ and $C_j < C_j(L2)$. As the value of C_j determines the forbidden areas for particle motion, a decrease in the value of C_j, will increase the region in which the particle can move. For example, if the value of C_j related to the motion of a particle is such that $C_j \geq C_j(L1) = 3.18834$, its orbit will always be around one of the primaries only. If $C_j(L2) \leq C_j < C_j(L1)$, the particle will be able to move around the two primaries, since the passage through L1 is open for $C_j < C_j(L1) = 3.18834$. Now, if $C_j < C_j(L2) = 3.17216$, the particle will be able to move around the two primaries and still escape from the Earth-Moon system through L2, since the passage through L2 is open for $C_j < C_j(L2)$.
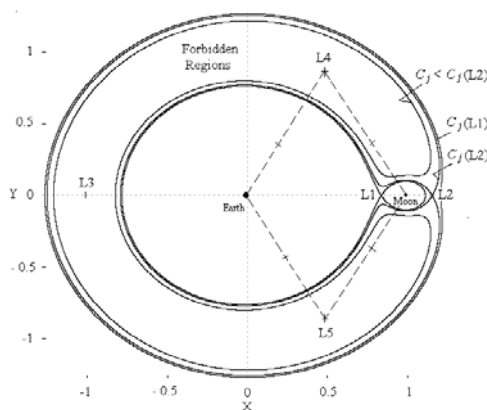
Figure 1. Lagrangian equilibrium points associated with the Earth-Moon-particle system in the frame rotating, and zero velocity curves for $C_j = C_j(L1)$, $C_j = C_j(L2)$ and $C_j = 3.1250 < C_j(L2)$.

2.2. The Four-body Sun-Earth-Moon-particle Problem

In a real mission, the Sun's gravitacional field, the eccentricity of the Earth's orbit, the eccentricity and the inclination of the Moon's orbit influence the probe's motion in transfer maneuvers between the Earth and the Moon. To assess these influences, the four-body Sun-Earth-Moon-probe problem must be considered.

If we associate the indexes 1 to the Sun, 2 to the Earth, 3 to the Moon and 4 to the particle of mass M_P such that, $\mu_1 = M_{Sun}/(M_{Earth}+M_{Moon})$, $\mu_2 = \mu_{Earth}$, $\mu_3 = \mu_{Moon}$ and $\mu_4 = M_P/(M_{Earth}+M_{Moon})$ are theirs reduced masses. Assuming that these four bodies move in three-dimensional space under only the action of their mutual gravitational attractions and an inertial Cartesian coordinate system (x, y, z) with origin in a fixed point of the space. Then, with $\mathbf{r}_i = (x, y, z)$ the vector position of one of the bodies in this system, the equations of motion of its are given by

$$\ddot{\mathbf{r}}_i = \sum_{\substack{j=1 \\ j \neq i}}^{4} \frac{\mu_j}{r_{ji}^3} (\mathbf{r}_j - \mathbf{r}_i)$$ (3)

where $r_{ij} = |\mathbf{r}_j - \mathbf{r}_i| = [(x_j - x_i)^2 + (y_j - y_i)^2 + (z_j - z_i)^2]^{1/2}$, with $j \neq i$, are the distance between ith and jth bodies. The Eq.(3) represents 12 second order differential equations and expresses the fact that the acceleration of a given body is the result of the of the sum of the forces exercised by the other three bodies. However, we assume that the particle not influences the motion of the other bodies. For this reason, the terms of Eq. (3) which contains μ_4 can be suppressed. We considered for four-body Sun-Earth-Moon-particle problem the same parameter of normalization of the previous subsection.

The eccentricity of the Earth's orbit ($e_{Earth} = 0.0167$), the eccentricity ($e_{Moon} = 0.0549$) and the inclination ($i_{Moon} = 5.1454°$, relative to the ecliptic) of the Moon's orbit are introduced to the system via initial conditions, thus bringing it ever closer to reality.

3. DEFINING THE ESCAPE AND CAPTURE ROUTES

3.1. Definition for the R3BP

According to the previous section, for the R3BP, the value of C_j of a given trajectory determines in the xy plane in synodic coordinate system allowed regions to the particle motion. Our goal is to consider this property to find sets of trajectories, which, upon escaping from the Moon, or being captured by it, through L1 and L2. These paths define natural routes that can be used in low-energy Earth-Moon and Moon-Earth transfers. For this purpose, we examined the lunar sphere of influence integrating trajectories in 1000 day periods (appropriate time for practical purposes) whose initial conditions in the synodic coordinate system have the following form

$$(x_0; y_0; \dot{x}_0; \dot{y}_0) = (x_0; 0; 0; \dot{y}_0) . \tag{4}$$

In order to determine the values of x_0 e $\dot{y}_0$ we consider firstly another Cartesian coordinate system with origin fixed in the Moon centre of mass (Selenocentric system), such that in $t = 0$, the x axis of this system coincides with x axis of the synodic system. Then, we define x_0 e $\dot{y}_0$ starting from four osculating orbital elements relative to the Moon in $t = 0$: semi-major axis a_0, eccentricity e_0, argument of periselenium w_0 measured in the xy plane starting from the x axis in direction of the probe's motion, and time of periselenium passage T_0. The other orbital elements: inclination i_0 relative to the Moon's orbital plane is equal to zero. As the orbits are coplanar, it is not necessary to define the longitude of the ascending node Ω_0, but it can be considered equal to zero and also measured starting from x axis in clockwise. Thus considering $1750\text{km} \leq a_0 \leq 66650\text{km}$, $0 \leq e_0 < 1$ and $T_0 = 0$ we can define two sets of direct trajectories. The first has $w_0 = 180^\circ$, therefore, with periselenium between L1 and the Moon, that is,

$$x_0 = \mu_{Earth} - a_0^*(1-e_0) \Rightarrow x(\text{L1}) \leq x_0 < (\mu_{Earth} - R_{Moon}^*) \tag{5}$$

$$\dot{y}_0 = -\left[\frac{\mu_{Moon}(1+e_0)}{a_0^*(1-e_0)}\right]^{1/2} + a_0^*(1-e_0) \tag{6}$$

The second set has $w_0 = 0^\circ$ and periselenium between the Moon and L2,

$$x_0 = \mu_{Earth} + a_0^*(1-e_0) \Rightarrow (\mu_{Earth} + R_{Moon}^*) < x_0 \leq x(\text{L2}) \tag{7}$$

$$\dot{y}_0 = \left[\frac{\mu_{Moon}(1+e_0)}{a_0^*(1-e_0)}\right]^{1/2} - a_0^*(1-e_0) \tag{8}$$

where $R_{Moon}^* = (R_{Moon} / 384400\text{km})$ is the average radius of the Moon ($R_{Moon} \approx 1738\text{km}$), and $a_0^* = (a_0/384400\text{km})$ is the semi-major axis of initial osculating lunar orbit, both in dimensionless system. The sets defined by Eq. (5) and (6) and by Eq. (7) and (8) were investigated separately. But, for the two sets, the semi-major axis and the eccentricity intervals of variation were swept with steps $\Delta a_0 = 550\text{km}$ and $\Delta e_0 = 0.008$. In this manner, we integrated 14632 trajectories from each of the sets.

The energy of two-body Moon-probe does not remain constant in the dynamical systems considered. Even so, monitoring of this quantity gives us a clear idea of the influence of the Moon's gravitational field on the trajectory. So, for each integrated trajectory, at each step of integration, we measured the Moon-probe energy. If it became positive during the integration, the trajectory is considered an escape trajectory and classified according to its time remaining around the Moon with negative energy, or simply capture time (Winter and Vieira Neto, 2002), and to whether its first escape occurs after L1 or L2.

The results of these integrations, for the R3BP, are shown in the plot of the eccentricity versus the semi-major axis of the initial osculating lunar orbit as a function of the capture time in the diagrams of Fig. 2 and 3. Figure 2 corresponds to the direct trajectories of the set defined by Eq. (5) and (6) whose periselenium are between L1 and the Moon, while the diagram in Fig. 3 corresponds to the trajectories with periselenium between the Moon and L2 defined by Eq. (7) and (8). Capture time was represented in different shades of gray, with each shade corresponding to the interval that the trajectory remains around the Moon with negative Moon-probe energy. The diagrams also show the initial conditions of trajectories that collide with the Moon.

In the diagram of Fig. 2(a), it is possible to identify four distinct regions, with three of them directly related to the values of C_j of the direct trajectories and, consequently, to the possibility or not of escape and capture through L1 and L2, and are shown limited by three lines. The first line, of the left for right, corresponds to the points of the diagram

whose initial conditions corresponding to (a_0, e_0) generate trajectories with $C_j = C_j(L1) = 3.18834$. So, the points to the left (including collision areas with the Moon located to the left of the first line) correspond to the initial conditions of the trajectories that have $C_j > C_j(L1)$ and, therefore, cannot escape from the Moon's sphere of influence. The second line, of the left for right, in turn, corresponds to points with $C_j = C_j(L2) = 3.17116$, thus, the points between it and the first line represents the initial conditions of trajectories that have $C_j(L2) < C_j < C_j(L1)$ and can escape from the sphere of lunar influence through L1, orbit the region around the Earth, and later be recaptured by the Moon. The third line is in the lower far right of the diagram of Fig. 2(a) and the points of this line also correspond to the initial conditions of trajectories with $C_j = C_j(L2)$. So, all initial conditions corresponding to (a_0, e_0) that represent points below this line have $C_j(L2) < C_j < C_j(L1)$ and, therefore, they can escape from the sphere of lunar influence through L1 and be recaptured by the Moon later. The points to the right of the second line and above the third line represent initial conditions of trajectories with $C_j < C_j(L2)$ and which can escape through L2 to outside the Earth-Moon System, or through L1 to the region around the Earth as verified in some cases. The fourth region mentioned refers to a region of stable orbits associated with periodic orbits of Family H2 and quasi-periodic orbits that oscillate around them (Winter and Vieira Neto, 2002; de Melo *et al.* 2005). This region is shown in the Fig. 2(b). Analysis of the diagram in Fig. 3 is similar; however, it does not present any regions of stable orbits of significant size.

In this way, we can define the escape and capture routes through L1 and L2 in a simple way based on the values of C_j found for initial conditions corresponding to (a_0, e_0). Thus, all those that have $C_j(L2) \leq C_j < C_j(L1)$ are escape and capture trajectories through L1. A typical trajectory in this set can be seen in Fig. 4. On the other hand, all those that have $C_j < C_j(L2)$ are escape and capture trajectories through L2, or L1. Figure 5 shows a typical trajectory of this set. The trajectories belonging to the region of stability between the first and second lines, showed in zoom in Fig. 2(b), also have $C_j(L2) \leq C_j < C_j(L1)$, but they do not escape through L1 for any time period below 1000 days (Winter and Vieira-Neto, 2002).

The routes we have just raised can be used as a convenient way to insert probes, without any insertion cost, around the Moon, taking advantage of the phenomenon of gravitational capture, or ballistic capture (Belbruno and Miller, 1990, 1993; Koon *et al.*, 2000, 2001). For example, by leading a probe to the trajectories shown in Fig. 4 or 5, it will be captured naturally by the Moon, remaining in this orbit for 700 and 40 days, respectively. These times are sufficient to perform a great number of missions. In addition, once captured, a small ΔV is sufficient to transfer the probe to a stable trajectory, thus allowing it to remain around the Moon for periods of up to 1000 days. On the other hand, it is possible to verify that in the Moon's sphere of influence, there is a superposition between the escape and capture routes through L1 and L2. This fact, in turn, raises the hypothesis that after being captured by the Moon (smaller primary mass) a probe can be guided at a low cost to an orbit around the Earth (larger primary mass). In this manner, if a dynamical structure similar to those shown in Fig. 2 and 3 repeats itself in other locations in the Solar System, the routes could also be used in low energy interplanetary missions.

3.2. Route analysis for the four-body problem

The properties of the escape and capture trajectories through L1 and L2 for the R3BP dynamics, especially the value of C_j, allow the definition of the routes. But, thinking about the use of the routes in real missions, it is important to verify which are the influences of the Sun's gravitational field, of eccentricity of the Earth's orbit and of the eccentricity and inclination of the Moon's orbit on them. So, we consider the four-body Sun-Earth-Moon-probe problem, as described in subsection 2.2, and we repeat the numerical simulations of the previous subsection. The influence of the Sun's gravitational field and the Earth and Moon's orbits were investigated together and also separately.
The results of these investigations show that the eccentricity of the Earth's orbit and the inclination of the Moon's orbit do not alter the structure of the points distribution of the graphs of Fig. 2 and 3. Therefore, they do not interfere in the
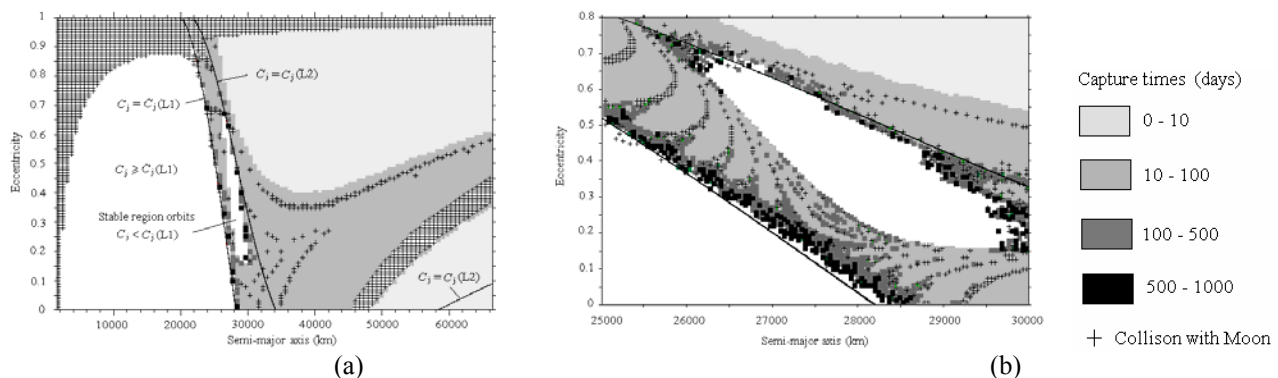
Figure 2. (a) Eccentricity versus semi-major axis of the initial osculating lunar orbit in terms of capture time indicated by the gray code for direct trajectories with periselenium between L1 and the Moon. (b) Zoom of the region of stable orbits associated with periodic orbits of Family H2 and quasi-periodic orbits that oscillate around them.
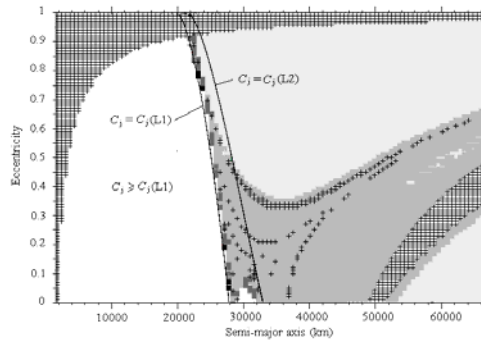
Figure 3. Eccentricity versus semi-major axis of the initial osculating lunar orbit in terms of capture time indicated by the gray code for direct trajectories with periselenium between the Moon and L2, for R3BP. Consider the same legend of de Fig. 2.

(a)   (b)
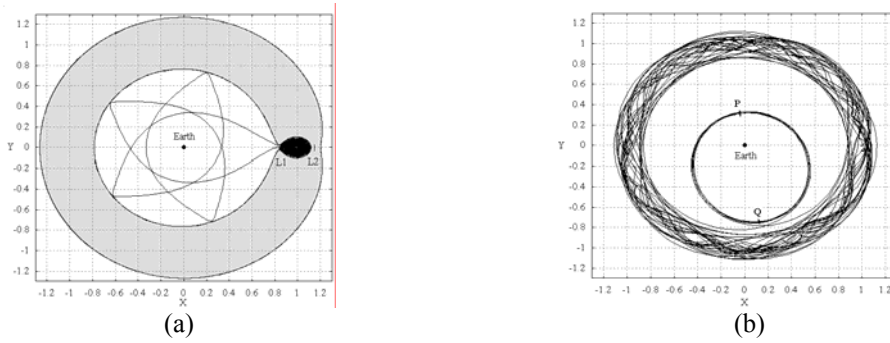
Figure 4. Typical trajectory of escape and capture through L1 seen in the coordinate: (a) synodic, and (b) geocentric systems.

(a)   (b)
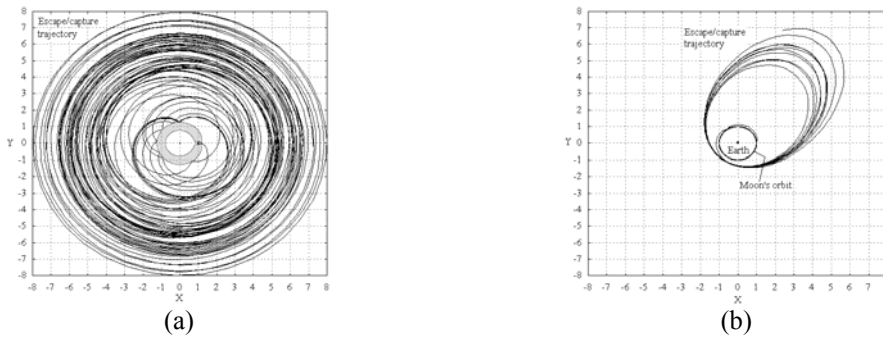
Figure 5. Typical trajectory of escape and capture through L2 seen in the coordinate: (a) synodic, and (b) Geocentric systems.

existence of the routes. On the other hand, the Sun's gravitacional field and the eccentricity of the Moon's orbit change the points distribution in the graphs, as we can see in Fig. 6 and 7 (de Melo *et al.* 2005). However, they do not destroy the internal and external routes. In general, the affects of the Sun's gravity and of eccentricity of the Moon's orbit do not impose restrictions to the acquisition maneuvers that we will study in the next section. The trajectories of the external route are affected by the Sun's gravity. After they escape through L2, they enter in heliocentric orbits, different from the observed for R3BP. Even so, the acquisition of these trajectories continue being possible.

In the diagrams of Fig. 6 and 7 the lines for which the initial conditions corresponding to (a_0, e_0) generate $C_j = C_j(L1)$ and $C_j = C_j(L2)$ are present. The Jacobi constant cannot be defined for the four-body problem. For this reason, their purpose is to facilitate the visualization of the differences between the points' distributions found for R3BP and the four-body problem. For R3BP these lines represent the exact borders among the permanent trajectories captured and the ones that escape and are recaptured through L1 and L2. For the four-body problem, the lines cannot be considered the exact border, but they allow us to understand the influence of the Sun's gravitational field and the eccentricity of the Moon's orbit on the trajectories while they are captured, especially on those belonging of the stability regions with $C_j \geq C_j(L1)$ and associated to the Family H2. The size of the white area on the left of the diagrams that represents the permanently captured trajectories is slightly reduced. The white area corresponding to the stable orbits associated with the Family H2 has its size reduced to 1/5 of the original as shown in Fig. 6(b). The escape and capture trajectories through L1 continue located between the white area and the area around the line $Cj = Cj(L2)$, and the escape and capture trajectories through L2 to the right of the line $Cj = Cj(L2)$.

<table>
<tr><td>(a)</td><td>(b)</td></tr>
</table>
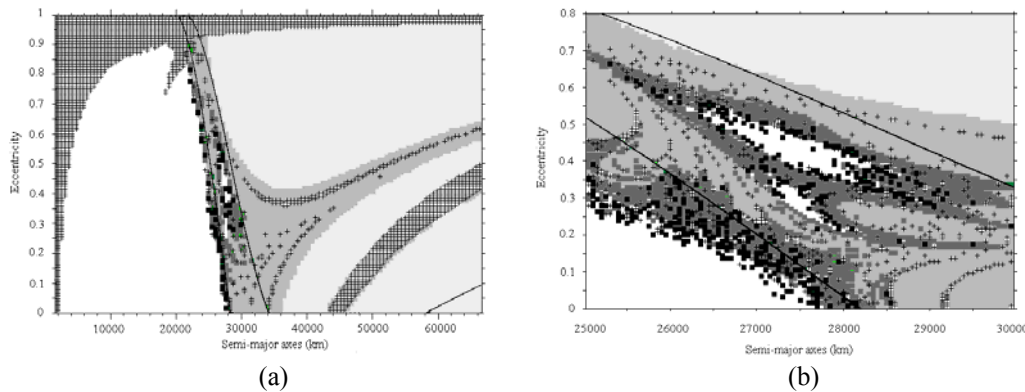
Figure 6. (a) Eccentricity versus semi-major axis of the initial osculating lunar orbit in terms of capture time indicated by the grey code for trajectories with periselenium between L1 and the Moon considering the four-body Sun-Earth-Moon-particle problem. (b) Zoom shows the region of stable orbits associated with periodic orbits of Family H2. Consider the legend of Fig. 2.
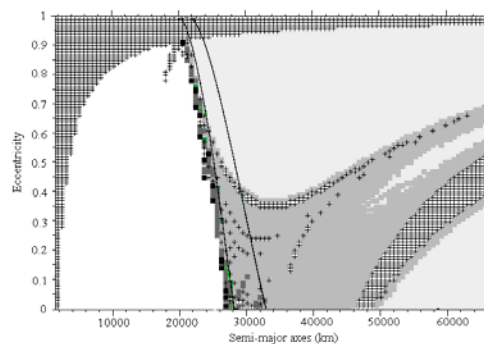
Figure 7. Eccentricity versus semi-major axis of the initial osculating lunar orbit in terms of capture time indicated by the gray code for trajectories with periselenium between the Moon and L2, considering the four-body Sun-Earth-Moon-particle problem. Consider the same legend of Fig. 2.

4. TRANSFER MEANS

4.1. General Description

The goal of this section is to present two procedures that allow the analysis of the acquisition costs of the capture route through L1 (internal route) and one for acquisition of the capture route through L2 (external route). For the internal route, we considered two maneuvers based on the Hohmann and bi-elliptic transfers. Conventionally, both are used to perform transfer maneuvers between concentric orbits starting from the application of two and three impulses to the space vehicle respectively, and they are totally described by the dynamics of the two-body problem. However, in our case, the final orbit will be a trajectory belonging to one of the routes. Figure 8 shows the maneuvers for internal route acquisition which will be described in the subsection 4.2. For external route acquisition, we consider a bi impulsive transfer initially conceived to be a geocentric ellipse with its apogee in the same area of the apogees of the route's trajectories, as shown in the Fig. 9, which will be described in the subsection 4.3.

The first step is to choose which is the best trajectory of the capture routes, or better set of them. This, obviously, will depend on the type of mission. It is through this choice that we can find the values of the velocity of the routes trajectory(ies) (magnitude and direction) in the area where the acquisition maneuver will be made and the distances where this maneuver will be made. With these information, we can calculate the apogee distance, semi-major axis, the energy, the perigee and apogee velocities of the transfer ellipses and the values of the impulses to perform the maneuver. The choice can be made through the graphs eccentricity versus semi-major axis in terms of the permanence time around the Moon of Fig. 2 and 3 or 6 and 7, and of the analysis of the chosen trajectories evolution out of the lunar sphere of influence to determinate the best area to perform the acquisition maneuver.

Then, the basic idea behind the three procedures consists of considering the two-body Earth-probe problem to obtain an analytical estimate of the ΔV_1 to launch the probe starting from a LEO (Low Earth orbit) in an ellipse; of the ΔV_2 (for maneuver based on the Hohmann transfer), or ΔV_2 and ΔV_3 (for maneuver based on the bi-elliptic transfer) necessary to insert it in a chosen routes trajectory(ies). In other words, to find the initial conditions to launch the probe and the acquisition point of the routes. With these established conditions by the two-body problem, we integrated the paths considering R3BP Earth-Moon-probe and the four-body Sun-Earth-Moon-Probe problem. The objective is to adjust the initial conditions and to determine eventual midway corrections to obtain a connection path between the LEO and a routes trajectory(ies).

The order of the events for routes acquisition maneuvers established considering the two-body Earth-probe problem, described in the previous paragraph, is the same when the maneuvers are analyzed considering R3BP and the four-body problem. The adjustments and midway corrections allow us to find close paths of the transfer ellipses conceived by the two-body Earth-probe problem, however, their apogees and perigees are not aligned with the Earth different from the observed for the Hohmann and bi-elliptic transfers (Fig. 8). Although these adjustments are small, they are essential for execution of the maneuver, because without them, the ellipses conceived by the two-body problem degenerate due to the action of the Sun's and Moon's gravitational fields.

In the moment of the application of ΔV_2 or ΔV_3, the knowledge of the routes becomes more important. Because, if ΔV_2 or ΔV_3 are not capable to place the probe exactly in the trajectory previously chosen to take it until the Moon, due to rockets imprecision, for example, it will place the probe in a close trajectory of that chosen. Once inside of the route, small ΔV (targeting) (Macau and Grebogi, 2006) can correct the failure in the acquisition moment and, then, to place the probe in the correct trajectory.
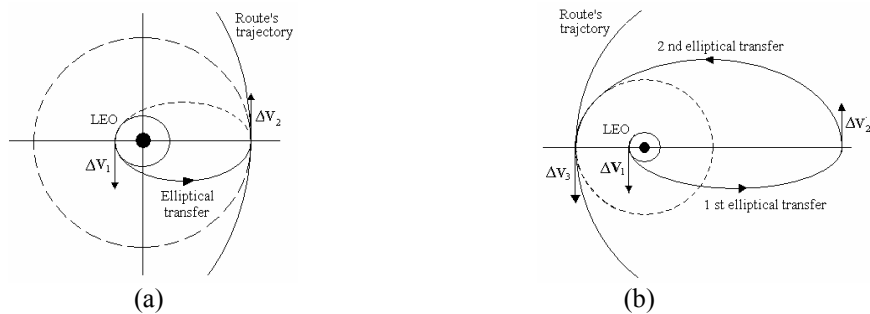
Figure 8. Basic geometry of transfers: (a) Hohmann, (b) bi-elliptic. Both adapted for acquisition of capture trajectories through de L1.

4.2. Means for acquisition of the internal route

The trajectories of this route stabilize themselves in non-Keplerians orbits around the Earth after they escape through L1. While they remain around the Earth, some of them reach altitudes about 40000km from the Earth's surface and, in general, they can reach the farthest distance from the Earth's surface between 290000km and 320000km, as can be seen in the trajectory of Fig. 10(a) whose initial conditions corresponds to $(a_0, e_0) = (33900\text{km}, 0.0000)$ and $Cj = 3.171644$. For this trajectory, the Earth-probe distance varies between 45260km and 310000km and it escapes and is recaptured by the Moon's gravity twice during the 1000 days of integration. What is observed for the trajectory of Fig. 10(a) also is observed for many other trajectories belonging to internal routes. This means that a probe could be inserted in these trajectories at any point whose distance from the Earth's surface is between 40000km and 320000km. Then, it would remain around the Earth until it is recaptured through L1, which could take a long time. But this procedure may not be interesting exactly because of the long transfer time. This problem can be solved by using targeting techniques to reduce the transfer time.
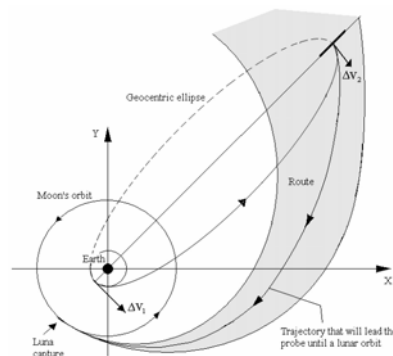
Figure 9. An illustration of defined escape/capture routes for trajectories that escape and are captured through L2 in geocentric coordinate system.

the Moon's gravity twice during the 1000 days of integration. What is observed for the trajectory of Fig. 10(a) also is observed for many other trajectories belonging to internal routes. This means that a probe could be inserted in these trajectories at any point whose distance from the Earth's surface is between 40000km and 320000km. Then, it would remain around the Earth until it is recaptured through L1, which could take a long time. But this procedure may not be interesting exactly because of the long transfer time. This problem can be solved by using targeting techniques to reduce the transfer time. On the other hand, in order to study transfers without the intensive use of targeting techniques, we can

consider the trajectories of the internal route during 10 days before they are recaptured by the Moon. This way, it is possible identify the limits of the final section of the internal route that will lead the probe until to the lunar sphere of influence directly as we can see in Fig. 10.(b).

Now, considering the two-body Earth-probe problem, the analytical estimate for ΔV_{Total} found for the acquisition maneuver based on the Hohamnn transfer at the points closest to the Earth's surface, in the final section of the internal capture route (points on PP' segment in Fig. 10.(b)), it exceeds 4.100km/s. Therefore, this maneuver is not economically viable. This was also verified for R3BP and the four-body problem. But if the route acquisition is performed in the points farther from the Earth's surface in the final section of the internal capture route, between 290000km and 320000km (points on QQ' segment in Fig. 10.(b)), the ΔV_{Total} values are smaller. The maneuver consists of applying two impulses. The first, ΔV_1, removes the probe from the LEO and place it in a geocentric ellipse that will take it to the distance between 290000km and 320000km from the Earth's surface. ΔV_1 is calculated just as in the conventional Hohmann transfer, that is, through the difference between the perigee velocity of the transfer ellipse and LEO velocity (supposed circular). The ΔV_1 value depends on the LEO's altitude and apogee radius of the transfer ellipse and its value is given by

$$\Delta V_1 = \left[2GM_{Earth} \left(\frac{1}{R_C} - \frac{1}{R_C + R_A} \right) \right]^{\frac{1}{2}} - \left[\frac{GM_{Earth}}{R_C} \right]^{\frac{1}{2}}, \tag{9}$$

where $G = 6.67 \times 10^{-20}$km/s^{2}kg is the gravitational constant, $M_{Earth} = 5.9742 \times 10^{24}$kg is Earth mass, $R_C = R_{Earth} + H_C$ is the LEO's radius, which is equal to the perigee's radius of the transfer ellipse, R_{Earth} is the average radius of the Earth ($R_{Earth} \approx 6370$km), H_C is the LEO's altitude given in km and R_A is the apogee's radius of the transfer ellipse, 290000km $\leq R_A \leq$ 320000km. A second impulse, ΔV_2, is applied to the probe to insert it in the route's trajectory that will take it until the Moon, and it is given by difference between the apogee velocity and velocity of the route's trajectory in the acquisition point. As we are considering that the acquisition maneuver is made in the farthest route point from the Earth (point **Q** in Fig. 4(b), for example) and that the transfer ellipse is tangent the route trajectory, we can also consider with good approach

$$\Delta V_2 = V_T - \left[2GM_{Earth} \left(\frac{1}{R_A} - \frac{1}{R_C + R_A} \right) \right]^{\frac{1}{2}}, \tag{10}$$

where V_T is the magnitude of vector velocity of the route's trajectory. For the set of trajectories with $C_j(L1) < C_j \leq C_j(L2)$, 0.600km/s $\leq V_T \leq$ 0.900km/s along the segment QQ' in Fig. 10.(b).

Considering a transfer leaving a LEO with an altitude of 200km, the ΔV_{Total} values of the maneuver vary between 3.660km/s and 3.780km/s, depending on the route trajectory chosen to lead the probe until to the Moon. The time required for acquisition maneuver varies between 3.4 and 3.9 days, and, once the acquisition is accomplished, the probe will be captured by the Moon within 10 days. The total time of the transfer varies, therefore, between 13 and 14 days.

The next step is to integrate the transfer paths between the LEO and the route considering the R3BP and the four-body problem. In this case, we verified that small adjustments in the values of ΔV_1 and ΔV_2 are necessary to performing the maneuver. With these adjustments the value of ΔV_{Total} passes to vary between 3.650km/s and 3.770km/s for the R3BP and 3.645km/s and 3.760km/s for the four-body problem.

On the other hand, the acquisition maneuver based on the bi-elliptic transfer made in the area between 290000km and 320000km from the Earth it is not economically viable. However, if it is performed at the area where the final section of the capture route trajectories is closest to the Earth's surface, between 110000km and 155000km, the costs are smaller. The first, ΔV_1, removes the probe from the LEO and launch it in a first transfer ellipse and it is calculated just as in the conventional bi-elliptic transfer, that is, through the difference between the perigee velocity of the first transfer ellipse and LEO velocity (supposed circular), and is given by

$$\Delta V_1 = \left[2GM_{Earth} \left(\frac{1}{R_C} - \frac{1}{R_C + R_{A1}} \right) \right]^{\frac{1}{2}} - \left[\frac{GM_{Earth}}{R_C} \right]^{\frac{1}{2}}, \tag{11}$$

where de R_{A1} is the apogee's radius of the first transfer ellipse. A second impulse, ΔV_2, is applied to the probe exactly in apogee of the first transfer ellipse and it places the probe in the second transfer ellipse, and it also is calculated just as in the conventional bi-elliptic transfer, that is, the difference between apogee velocities of the second and first transfers' ellipses

$$\Delta V_2 = \left[2GM_{Earth} \left(\frac{1}{R_{A2}} - \frac{1}{R_{A2} + R_{P2}} \right) \right]^{\frac{1}{2}} - \left[2GM_{Earth} \left(\frac{1}{R_{A1}} - \frac{1}{R_C + R_{A1}} \right) \right]^{\frac{1}{2}}, \tag{12}$$

where R_{P2} and R_{A2} are the perigee and apogee radius of the second transfer ellipse, respectively, with $110000\text{km} \leq R_{P2} \leq 155000\text{km}$. Note also that $R_{A2} = R_{A1}$. In the perigee of the second ellipse a third impulse, ΔV_3, is applied to insert the probe in a route trajectory. In this case, the acquisition is made in closest route point to the Earth (along the segment PP' in Fig. 10(b)), and by analogy with the anterior procedure, we can considerer

$$\Delta V_3 = V_T - \left[2GM_{Earth}\left(\frac{1}{R_{P2}} - \frac{1}{R_{A2} + R_{P2}} \right) \right]^{1/2}, \qquad (13)$$

where $2.180\text{km/s} \leq V_T \leq 1.800\text{km/s}$ is the route trajectory velocity along the segment PP' in Fig. 10(b).

The values of ΔV_{Total} leaving from a LEO with altitude of 200km vary between 3.540km/s and 3.590km/s depending on the trajectory, and the time required for acquisition maneuver is between 10 and 11 days. The capture by the Moon happens between 6 and 7 days after the route acquisition. Therefore, the total time transfer varies between 16 and 18 days.

The analysis of this acquisition maneuver also considering R3BP and the four-body problem show that small adjustments in the values of the three impulses are enough to conclude the maneuver. With these adjustments, the values of ΔV_{Total} vary between 3.510km/s and 3.575km/s for the R3BP and 3.505km/s and 3.565km/s for the four-body problem.

These results show that the two-body problem offers a good approach for the value of ΔV_{Total} of the acquisition maneuver, independent of the studied procedure. However, the analysis of the mission should consider more complex and realistic dynamical systems.

Once captured, the trajectories belonging to the route can remain around the Moon between 10 and 1000 days, see Fig. 2 and 3. These are non-Keplerians orbits, but some of them pass at few dozens of kilometers of the lunar surface. It is also interesting to notice, that the application of a small ΔV to the probe, after the capture, is enough to place it permanently in orbit around the Moon, being it a stable orbit associated to the Family H2 or one of the ones that have $Cj > Cj(L1)$.

(a)   (b)
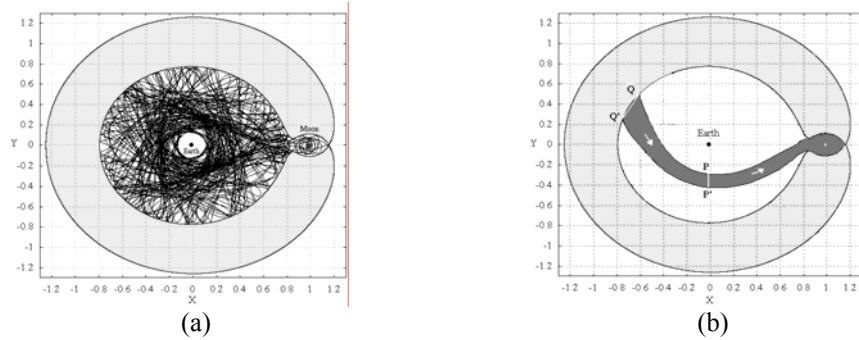
Figure 10. (a) Trajectory with initial condition relative to the Moon corresponding to $(a_0, e_0) = (33900\text{km}, 0.0000)$ and $Cj = 3.171644$, which Earth-probe distance after the escape varies between 45260km e 320000km. (b) Internal capture route defined for integration of the trajectories during 10 days before the capture by the Moon. Both in synodic coordinate system.

4.3. Means for acquisition of the external route

The trajectories of this route stabilize themselves in orbits around the Earth after they escape through L2, as show Fig. 5. Depending on the trajectory, the apogee distance varies between $4\times10^5\text{km}$ and 10^7km, considering the R3BP. In order to visualize the external capture route, it is necessary to consider an initial conditions corresponding to a (a_0, e_0) in diagrams of Fig. 2 and 3 or 6 and 7, for which $C_j < C_j(\text{L2})$. Then, we define an interval with radius ε centered in (a_0, e_0). For a small ε all trajectories in this interval will have similar evolution after they escape through L2. So, we can find capture routes like that shown in Fig. 9, which is obtained considering an interval around the trajectory of Fig. 5.

Then, considering the two-body problem firstly, we conceived a geocentric ellipse whose apogee is tangent to the route trajectory(ies). The maneuver consists of applying an impulse, ΔV_1, to launch the probe in this ellipse starting from the LEO given by

$$\Delta V_1 = \left[2GM_{Earth}\left(\frac{1}{R_C} - \frac{1}{R_C + R_{AE}} \right) \right]^{1/2} - \left[\frac{GM_{Earth}}{R_C} \right]^{1/2}, \qquad (14)$$

where R_{AE} is the perigee's radius of the transfer ellipse. A second impulse, ΔV_2, is applied to the probe in the opposite direction of its motion when it reaches the apogee of the ellipse with the objective of slow it down and to insert it in one route trajectory. Once again, we are considering that the acquisition maneuver is being made in a point where the transfer ellipse is tangent the route trajectory. However, we can also consider the approach

$$\Delta V_2 = \left[2GM_{Earth} \left(\frac{1}{R_{AE}} - \frac{1}{R_C + R_{AE}} \right) \right]^{\frac{1}{2}} + V_T , \qquad (15)$$

where V_T is the apogee velocity of the route trajectory. With the application of ΔV_2, the probe is inserted in the route and, starting from this instant, it will follow the opposite sense (direction) to the taken by the paths after the escape, that is, the integration will be made for backward in time. For the apogees about 1.5×10^6km, the ΔV_{Total} of the maneuver varies between 3.530km/s and 3.590km/s when the probe is launched of a LEO with altitude of 200km, and the time of the acquisition maneuver is between 37 and 38 days, depending of the trajectory. The capture happens between 62 and 64 days after the acquisition. This is verified for any trajectories whose initial conditions corresponding to (a_0, e_0) furnishes a $C_j < C_j$(L2) in Fig. 2 and 3 or 6 and 8. Therefore, the total transfer time is between 99 and 101 days. For the apogees about 2.0×10^6km, the ΔV_{Total} of the maneuver varies between 3.430km/s and 3.460km/s, time of the acquisition maneuver is between 58 and 59 days and the capture happens between 100 and 101 days. Therefore, the total transfer time is between 159 and 160 days. Fig. 9 shows an illustration of this maneuver.

Similarly to the made for the internal route, the initial conditions established for the two-body problem were integrated for R3BP and the four-body problem. Following the observed for the other procedures, small adjustments allow finding the closest path of the Real. With these adjustments, the ΔV_{Total} of the maneuver varies between 3.510km/s and 3.570km/s for acquisition to 1.5×10^6 km of the Earth and between 3.420km/s and 3.450km/s for acquisition to 2.0×10^6 km. The time continues the same. Once again, the results show that the two-body problem can be considered to determine the ΔV_{Total} of the maneuver with good approach.

5. CONCLUSIONS

In this work, we presented two set of trajectories starting from which it is possible to define two natural routes of capture by the Moon through L1 and L2. The routes were defined considering properties of R3BP, but their existence also was verified for the four-body Sun-Earth-Moon-probe problem.

A study on some maneuvers based on the Hohmann and bi-elliptic transfers for the routes acquisition also were presented. With respect to the acquisition of the internal route, the maneuver based, for example, on the bi-elliptic transfer allows to insert a probe in a Moon orbit without the need of impulses for this end, with 3.540km/s $\leq \Delta V_{Total} \leq$ 3.590km/s, for a probe leaving a LEO with altitude of 200km and total transfer time between 16 and 18 days. After the capture, the trajectories remain in orbits of the Moon for periods that can vary between 10 and 1000 days and, still, smalls ΔV can move them to permanent orbits, as the stable orbits associated to the Family H2, or those located in the area of stability with $Cj > Cj$(L1). Thus, a great number of future transfers missions followed by permanence around the Moon can take advantage of this route; be them automatic or manned missions, since the transfer lasts on average only 2.5 weeks. The ΔV_{Total} for acquisitions maneuver of the external route varies between 3.550km/s and 3.570km/s for acquisition at 1.5×10^6km from the Earth and between 3.440km/s and 3.470km/s for acquisition at 2.0×10^6km from the Earth and the total time of these transfers are about 100 and 160 days, respectively, and both for a probe leaving a direct LEO with altitude of 200km. The effects of Sun's gravitational field, the eccentricity of the Earth's orbit and the eccentricity and inclination of the Moon's orbit don't impose restrictions to the acquisition maneuvers for these routes.

Given the exposed, we can conclude that the routes presented here represent good options for a great number of future missions destined to the Moon face the economy that they can provide, without require times of transfer very long, as in the case of the maneuver based on the bi-elliptic transfer.

In future studies, there may be methods that make acquisition of the capture routes with even smaller ΔV_{Total} specially with targeting techniques. On the other hand, the structure found in the mapping of the lunar sphere of influence showing escape and capture trajectories may exist, in a similar way, in other localization of the Solar System, and exploration of these trajectories may also be useful in future interplanetary missions.

6. ACKNOWLEDGEMENTS

7. REFERENCES

Arenstorf, R.F., 1963a, "Existence of Periodic Solutions Passing Near Both Mass of Restricted Three-Body Problem", AIAA J. 1 (1), 238-240.

Arenstorf, R.F., 1963b, "Periodic Solutions of Restricted Three-Body Problem Representing Analytic Continuations of Keplerian Elliptic Motions", Am. J. Math. 85, 27-35.

Bate, R.R., Mueller, D.D., White, J.E., 1971, "Fundamentals of Astrodynamics", Dover Publications Inc.

Belbruno, E.A. Lunar Capture Orbits, 1997, "A Method of Constructing Earth Moon Trajectories and the Lunar Gas Mission". Proceedings of 19th AIAA/DGLR/JSASS International Electric Propulsion Conference, AIAA-87-1054.

Belbruno E.A., Miller J.K., 1990, "A Ballistic Lunar Capture Trajectory for Japanese Spacecraft Hiten", JPL, IOM 312/90.4-1731.

Belbruno, E.A., Miller, J.K., 2005, "Sun-Perturbed Earth-to-Moon Transfers with Ballistic Capture", J. Guid. Control Dynam. 16 (4), 770-775.

Broucke, R.A., 1968, "Periodic Orbits in the Restricted Three-Body Problem with Earth-Moon Masses". JPL, Technical Report 32-1168.

Dahlke, S.R., 2003, "Lunar Gravitational Capture Conditions", J. Guid. Control Dynam. 26 (4), 635-642.

Davidson, M.C., 1964, "Numerical Examples of Transition Orbits in Restricted Three-Body Problem", Acta Astronaut. 10 (308), 308-313.

de Melo, C.F., Winter, O.C., Vieira Neto E., 2005, "Numerical study of low cost alternative orbits around the Moon", Adv. Space Res. 36 (3), 552-560.

Koon W.S., Lo, M.W., Marsden, J.K., Ross, S.D., 2000, "Heteroclinic Conections between Periodic Orbits and Resonance Transition in Celestial Mechanics", Chaos 10 (2), 427-469.

Koon W.S., Lo, M.W., Marsden, J.K., Ross, S.D., 2001, "Low Energy Transfer to the Moon", Celest. Mech. Dyn. Astr. 81 (1), 63-73.

Macau, E.E.N., Grebogi, C., 2006, "Control of chaos and its relevancy to spacecraft steering", Phil. Trans. R. Soc. A, 364, 2463-2481.

Murray, C. D. and Dermott, S. F., 1999, "Solar System Dynamics". UK: Cambridge University Press.

Villac, B.F., Scheeres, D.J., 2003, "Escaping Trajectories in the Hill Three-body Problem and Applications", J. Guid. Control Dynam. 26 (2), 224-232.

Winter, O.C., Vieira Neto, 2002, E. "Distant Stable Direct Orbits Around the Moon", A&A 393, 661-671.

8. RESPONSIBILITY NOTICE

The authors are the only responsible for the printed material included in this paper.